Author/s:
Georgiou, DC;Haghighatbin, MA;Hogan, CF;Scholz, MS;Bull, JN;Bieske, EJ;Wilson, DJD;Dutton, JL

Title:
A Strong cis‐Effect in an Imidazole‐Imidazolium‐Substituted Alkene

Date:
2017-07-10

Citation:
Georgiou, D. C., Haghighatbin, M. A., Hogan, C. F., Scholz, M. S., Bull, J. N., Bieske, E. J., Wilson, D. J. D. & Dutton, J. L. (2017). A Strong cis‐Effect in an Imidazole‐Imidazolium‐Substituted Alkene. Angewandte Chemie, 129 (29), pp.8593-8600. https://doi.org/10.1002/ange.201702287.

Title: A strong cis-effect in an imidazole-imidazolium substituted alkene

Authors: Jason Laurence Dutton; David Wilson

To be cited as: 10.1002/ange.201702287

Link to VoR: https://doi.org/10.1002/ange.201702287

A strong cis-effect in an imidazole-imidazolium substituted alkene

Dayne C. Georgiou,[a] Mohammad A. Haghighatbin,[a] Conor F. Hogan,[a] Michael S. Scholz,[b] James N. Bull,[b] Evan J. Bieske,[b] David J. D. Wilson[a] and Jason L. Dutton[a]**

[a] Department of Chemistry and Physics, La Trobe Institute for Molecular Science, La Trobe University, Melbourne, Victoria 3086, Australia

[b] School of Chemistry, University of Melbourne, Parkville, Victoria 3010, Australia

ABSTRACT

We report the first example of an alkene with two carbon bound substituents (imidazole and imidazolium rings) where the Z-isomer has a greater thermodynamic stability than the E-isomer which persists in both the gas phase and in solution. Theoretical calculations, solution fluorescence spectroscopy and gas-phase ion mobility mass spectrometry studies confirm the preference for the Z-isomer, the stability of which is traced to a non-covalent interaction between the imidazole lone pair and the imidazolium ring.

Key Words

Conformation Analysis – Nitrogen Heterocycles – cis-effect

Introduction

The greater thermodynamic stability of E-stillbene **1** (and E-disubstituted alkenes in general) over the Z-isomer, and the thermal/photoisomerism between the two forms, are concepts taught to virtually every chemistry student. Cases where the cis- or Z-isomer has greater thermodynamic stability are rare, mostly limited to di-halo (e.g. **2**) or dimethoxy alkenes (e.g. **3**), monohalo-propenes and 2-cyanopropene with strong electron withdrawing atoms/groups are directly bound to the alkene. The phenomenon has been coined "the cis-effect" and the underlying rationale for the effect has been the subject of study over the last fifty years.[1] Allyl anions also adopt a Z-configuration, particularly when coordinated to a metal counter-cation, however calculations suggest that the Z-configuration is also preferred in the gas-phase anion.[2]

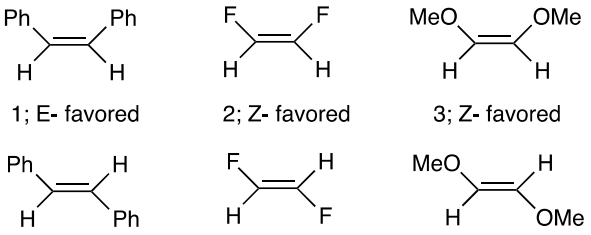

For difluoroethylene the Z-isomer is calculated to be more stable than the E-isomer by 4.5 kJ/mol at the CCSD(T) level, while the effect is somewhat weaker in the other cases.[1i] The most recent proposals suggest the origin of the cis-effect in difluoroethylene arises from a greater correlation energy of the Z-isomer in combination with steric attractions between the σ and π-type lone pairs on F atoms present in the Z-isomer.[1j]

Here we report on the first example of a non-cyclic alkene bearing two carbon atom bound groups (a benzimidazole and benzimidazolium ring) where the Z-isomer is more thermodynamically stable than the E-isomer and demonstrate that non-covalent interactions between the benzimidazole and benzimidazolium ring is the most important factor in stabilizing the Z isomer.

Computational Methods

All geometry optimizations were carried out in the gas phase with the B3LYP density functional[3] and 6-311++G(d,p) basis set[4] within Gaussian 09.[5] Stationary points were characterized as minima by calculating the Hessian matrix analytically at this level of theory. For comparison, geometries were optimized with B3LYP-D3(BJ),[6] yielding deviations of less than 0.005 Å in calculated bond distances to the B3LYP geometry. Molecular orbitals (MO) and natural bond orbitals (NBO) were calculated at the B3LYP/6-311++G(d,p) level of theory. NBOs were calculated with the NBO 5.9 program.[7]

Single-point energies were calculated at the B3LYP/6-311++G(d,p) gas phase geometries. DFT (including TD-DFT) and HF calculations were carried out within Gaussian 09,[5] with solvent effects employing a PCM approach[8] with Truhlar's SMD model with acetonitrile.[9] DLPNO-CCSD(T)[10] calculations with the cc-pVXZ (X = D, T) basis sets[11] were carried out within Orca 3.0.3.[12] Solvent effects for DLPNO-CCSD(T) were calculated with the COSMO solvent model[13] with acetonitrile.

Excited-state geometry optimisations for **6** were carried out within Molpro[14] using CASSCF(4,5) with a 6-31+G(d) basis set. Larger active spaces yielded equivalent results. Both the S_0 (ground state) and S_1 (first excited) states were calculated, with geometry optimizations utilising default routines.

Quantum theory of atoms in molecules (QTAIM) analysis[15] employed MP2/aug-cc-pVTZ electron densities at the B3LYP/6-311++G(d,p) geometries within Gaussian, with QTAIM analysis carried out with AIMALL.[16] Plots of QTAIM analysis were carried out within ADF[17] at the BP86/TZ2P level of theory with uncontracted Slater-type orbitals (STOs) as basis functions[18] and density.[19] Scalar relativistic effects have been incorporated by applying the zeroth-order regular approximation in all ADF calculations.[20] SAPT0 analysis was carried out within PSI 4,[21] with a jul-cc-pVDZ basis set[22] together with density fitting.

3. Results and Discussion

Synthesis and Characterization

Our group has studied the use of N-heterocyclic carbenes (NHCs) to stabilize small carbon-based fragments, including C_2.[23] The synthetic pathway to NHC^{Me}-stabilized C_2 (NHC^{Me}–C_2H_2–NHC^{Me}) requires the initial synthesis of bis-imidazole substituted ethylene **4** (Scheme 1),[23b] followed by dimethylation of complex **4**, giving dication **5**. If only one equivalent of MeI is used in the methylation of **4**, the ^{1}H NMR spectrum shows evidence for a compound with different rings, consistent with an imidazole/imidazolium trimethyl cation **6**.

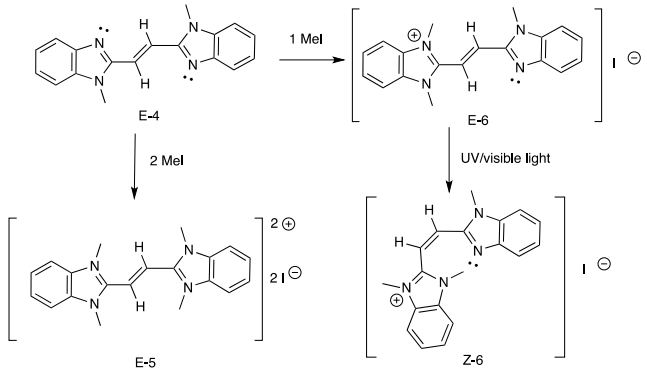

Scheme 1. Syntheses of **5, E-6** and **Z-6** from **4**.

Leaving a sample of **6** in an NMR tube (CD_3CN solution) on the laboratory bench for a few hours resulted in a color change from bright yellow to pale yellow. A ^{1}H NMR spectrum of the pale yellow sample indicated the presence of a second compound in addition to **6**. After being left to stand for three more hours the color faded further to very pale yellow and only ^{1}H NMR signals from the new compound were observed. Samples of **6** protected from light did not undergo any change, suggesting exposure to light is responsible for the reaction. Both **6** and the new compound had very low solubility in CD_3CN. To generate a derivative of **6** with improved solubility, a metathesis reaction with AgOTf was carried out on freshly methylated material in the dark. The ^{1}H NMR spectrum of the resulting more soluble material gave the same proton signals as the original compound **6**, and exposure to ambient light

in the NMR tube again resulted in the generation of the new compound. Single crystals of both compounds were grown in the dark. X-ray structures revealed the "original" bright yellow compound to be the E-isomer of the trimethyl cation (**E-6**, Figure 1) and the "new" pale yellow compound formed upon exposure to light to be the Z-isomer (**Z-6**, Figure 2). This cation had been reported over 50 years ago,[20,21] however the tendency towards isomerization was not observed in these early studies.

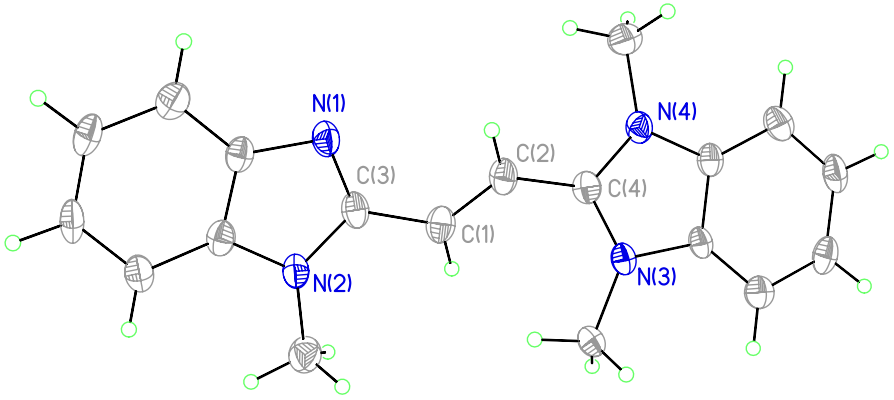

Figure 1. Crystal structure of **E-6**. Thermal ellipsoids are displayed at the 50% probability level and $[CF_3SO_3]^-$ is omitted. Selected bond distances (Å) [B3LYP/6-311++G(d,p) calculated]: C(1)-C(2) 1.334(5) [1.359], C(1)-C(3) 1.456(5) [1.437], C(2)-C(4) 1.444(5) [1.432].

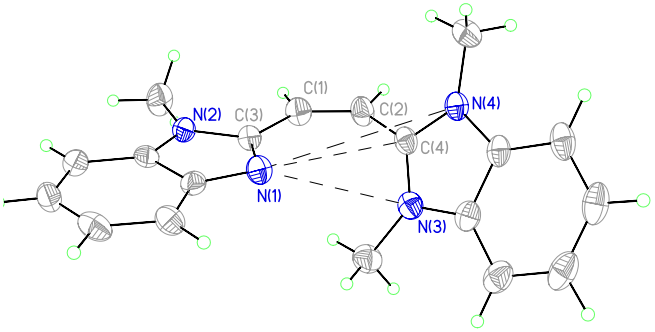

Figure 2. Crystal structure of **Z-6**. Thermal ellipsoids are displayed at the 50% probability level and $[CF_3SO_3]^-$ is omitted. Selected bond distances (Å) [B3LYP/6-311++G(d,p) calculated]: C(1)-C(2) 1.322(6) [1.348], C(1)-C(3) 1.439(5) [1.445], C(2)-C(4) 1.458(6) [1.467], N(1)-C(4) 3.078(5) [2.895], N(1)-N(4) 4.063(4) [3.614], N(1)-N(3) 3.118(4)[3.114].

The bond distances in the two structures are all as expected, and are generally well reproduced by calculations. For **E-6** the imidazole and imidazolium rings are slightly tilted from planarity relative to one another, while the ring systems are coplanar in **E-4**, and nearly perpendicular in **E-5**. For **Z-6** the crystal structure shows the two rings in a *gauche* arrangement, suggestive of a weak intramolecular bonding interaction between an imidazole nitrogen atom lone pair and the closest C and N atoms from the imidazolium ring that are within the sum of the van der Waals radii; the N(1)-C(4) and N(1)-N(3) separations are 3.078 and 3.118 Å, respectively. The B3LYP/6-311++G(d,p) calculated inter-ring N(1)-C(4) and N(1)-N(3) distances are slightly shorter at 2.895 Å and 3.114 Å, respectively. Inclusion of dispersion with B3LYP-D3(BJ)/6-311++G(d,p) further shortens the interactions to 2.787 and 3.009 Å, respectively. In contrast, dispersion only has a minimal effect on the central C=C bond distance (< 0.004 Å for **6**), which indicates that the intramolecular bonding interaction from the imidazole N may be considered a non-covalent interaction. The nature of the interaction is considered in detail below.

Isomerization

Having observed E to Z isomerization, we undertook experiments to determine the conditions under which isomerization occurs. Exclusion of light from the NMR sample resulted in no **E-6** to **Z-6** isomerization. Heating a solution of **E-6** protected from light did not produce a measurable change as monitored by ^{1}H NMR spectroscopy. Exposure of the **E-6** in CD_3CN solution to 354 nm UV light resulted in more rapid conversion from **E-6** to **Z-6**, with the formation of a 5:1 ratio of Z:E after 30 minutes of UV exposure. The same ratio is obtained whether starting from pure **E-6** or **Z-6**. Complete conversion to **Z-6** occurs on letting the NMR sample stand in ambient light for 1 hour. It was noticed that solutions of **Z-6** and **E-6** fluoresced in the green on exposure to 354 nm UV. Fluorescence under UV had been mentioned in the initial reports on the compound, but no further details given.[24]

Relative Stabilities of Isomers

The relative stability of gas-phase **E-6** and **Z-6** ions was characterized using a custom tandem ion mobility mass spectrometer.[25] Briefly, samples of either **E-6** or **Z-6** dissolved in methanol, when electrosprayed, gave arrival time distributions (mobility spectra) with one predominant peak, consistent with a single isomer (Figure 3a). The peak from the **E-6** solution has a longer arrival time than that from the **Z-6** solution, which is consistent with a more extended structure.[26] Irradiation of **E-6** solution with 385 nm light prior to analysis resulted in an arrival time distribution identical to that from pure **Z-6** solution, whereas illumination of **Z-6** solution yielded no discernible change in arrival time distribution. These results are consistent with the ^{1}H NMR characterizations described above. In a next set of measurements each isomer was isolated and subjected to collisional activation.[27] At higher collision energies a gas-phase quasi-equilibrium is established whereby the more stable isomer is more abundant.[28] Relative abundances of **E-6** and **Z-6** as a function of electric field in the collision zone are shown in Figure 3b and 3c, respectively. Regardless of the initially selected isomer (**E-6** or **Z-6**), at the quasi-equilibrium conditions **Z-6** is more abundant than **E-6**, providing evidence for the greater stability of the **Z-6** isomer in the gas phase.

In a separate set of ion mobility measurements, selected gas-phase **E-6** or **Z-6** isomers were irradiated with a wavelength tunable laser beam while monitoring the photoisomer signal to generate photoisomerization action (PISA) spectra (Figure 4). The PISA spectrum for **E-6** → **Z-6** has a maximum at ~420 nm, whereas the maximum of the **E-6** → **Z-6** PISA spectrum is blue-shifted to ~340 nm.

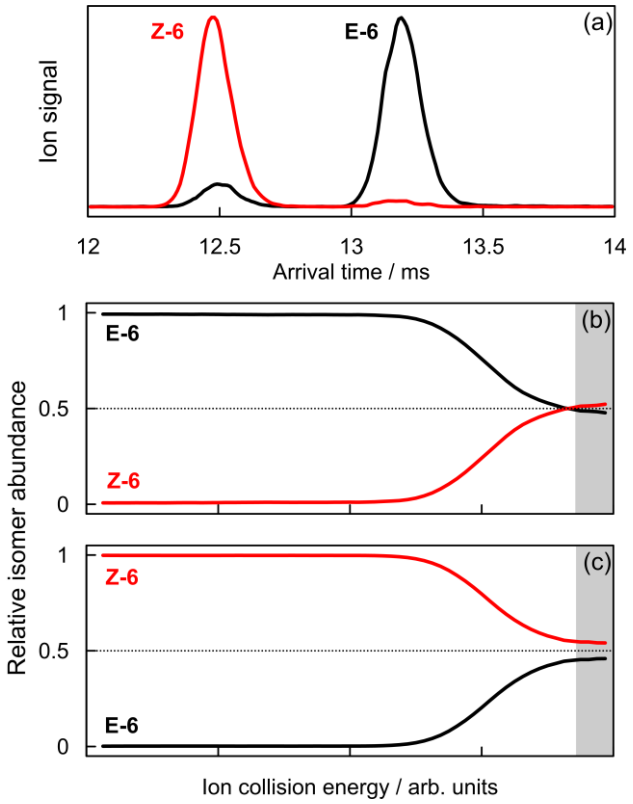

Figure 3. Ion mobility mass spectrometry: (a) arrival time distributions from **E-6** (black) and **Z-6** (red) solutions showing the two isomers can be clearly distinguished; (b) and (c) collisional activation of **E-6** and **Z-6** isomers, respectively. The quasi-equilibrium region is shaded grey.

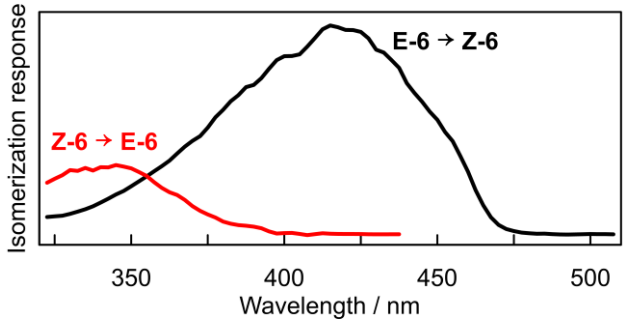

Figure 4. Gas-phase photoisomerization action spectra of **E-6** (black) and **Z-6** (red).

Calculated Relative Energies

The relative stability of E and Z isomers of **4**-**6** were explored with *ab initio* methods (Table 1). The relative energies are sensitive to computational method and solvent effects, which is particularly evident with **6**. For both **4** and **5**, all methods predict the E isomer to be favoured, consistent with experimental observations. The situation is quite different for **6**, largely due to the significant solvent effect (-16.7 kJ/mol with B3LYP/6-311++G(d,p)) in comparison with **4** (+1.2 kJ/mol) and **5** (+8.1 kJ/mol). In each case the solvent contribution is opposite in sign to the preferred isomer.

Analysis of results provides initial insight into the Z isomer preference in **6**. It is notable that for each of **4**-**6**, dispersion (D3 with Becke-Johnson damping) favours the Z isomer by 8-12 kJ/mol, which suggests that dispersion interactions (or non-covalent interactions generally) are a significant factor. The role of charge transfer was assessed by varying the contribution of Hartree-Fock exchange in the density functional, including BP86 (no HF exchange), B3LYP (20%), PBE0 (25%), CAM-B3LYP (19-65%) and ωB97X-D (22.5-100%) functionals with the 6-311++G(d,p) basis set. It could be expected that increasing the proportion of HF exchange would most effect systems with significant charge transfer characteristics.[29] For difluoroethylene, relative energies between Z and E vary by less than 1 kJ/mol for this set of functionals, indicative of the small role that charge transfer plays in difluoroethylene. For **4**-**6**, an increase in HF exchange increases the preference for Z, suggesting that pure DFT (self-interaction error leads to overestimation of electron density delocalization) actually favours the E isomer, whereas localization (with HF exchange) favours the Z isomer. As a measure of the effect, the difference between BP86 (0% HF exchange) and ωB97-XD (22.5-100%) relative energies (increasing the preference for Z) varies from +12.7 kJ/mol (**4**) to +18.7 kJ/mol (**5**) to +22.4 kJ/mol (**6**), which suggests that charge-transfer is significant in each system, and most important for **6**.

Table 1. Calculated relative energies (kJ/mol) of Z and E forms of **4**-**6**. Relative energies are calculated as E_e(E) - E_e(Z), with positive values indicating the Z isomer to be lower in energy. [a]

Method	Basis set	Conditions	**4**	**5**	**6**
B3LYP	6-311++G(d,p)	Gas phase (ΔE)	-31.96	-30.10	2.58
		ΔG_{corr}	-6.70	-0.79	-0.34
		MeCN (PCM)	-37.47	-22.81	-14.44
B3LYP-D3(BJ)	6-311++G(d,p)	Gas phase	-22.47	-18.22	10.69
BP86	6-311++G(d,p)	Gas phase	-31.84	-31.15	-1.62
PBE0	6-311++G(d,p)	Gas phase	-29.57	-26.41	5.68
CAM-B3LYP	6-311++G(d,p)	Gas phase	-28.44	-25.10	11.90
ωB97X-D	6-311++G(d,p)	Gas phase	-19.16	-12.49	20.80
HF	6-311++G(d,p)	Gas phase	-31.42	-23.13	19.29
DF-MP2-F12	cc-VDZ-F12	Gas phase	-17.63	-14.67	19.87
DF-SCS-MP2-F12	cc-VDZ-F12	Gas phase	-22.66	-20.79	16.38
DLPNO-CCSD	cc-pVTZ	Gas phase			26.12
DLPNO-CCSD(T)	cc-pVTZ	Gas phase			25.77
DLPNO-CCSD	cc-pVTZ	MeCN (COSMO)	-15.87	-9.31	10.67
DLPNO-CCSD(T)	cc-pVTZ	MeCN (COSMO)	-14.16	-7.88	10.64
PWPB95-D3BJ	def2-TZVP	Gas phase			13.71
PWPB95-D3BJ	def2-TZVP	MeCN (COSMO)			0.32

[a] Calculated at the B3LYP/6-311++G(d,p) optimized geometries. All results are electronic energies (ΔE) unless noted. MeCN = acetonitrile solvent, calculated with a PCM solvent model or COSMO solvent model.

Higher-level wave function methods serve to overcome the limitations of the HF approach. At the highest level of theory considered, DLPNO-CCSD(T)/cc-pVTZ inclusive of acetonitrile solvent (COSMO model), the **Z-6** isomer is more stable than **E-6** by 10.6 kJ/mol (gas phase is 25.8 kJ/mol). Analogous calculations for **4** and **5** predict the E-isomer to be more stable by 14.2 and 7.9 kJ/mol, respectively. For comparison, at the same level of theory the Z-isomer of difluoroethylene is more stable by 5.5 kJ/mol (gas phase 2.8 kJ/mol). Increasing the basis set to cc-pV5Z gives a gas-phase value of 4.2 kJ/mol, equivalent to the CCSD(T) complete basis set limit value reported by Feller.[1i] While compounds **4**-**6** are significantly larger than difluoroethylene and diffuse functions have not been included, it may still be expected that the DLPNO-CCSD(T) results for **4**-**6** are sufficiently accurate to provide a reliable preference for E or Z isomers.

Molecular Orbital and Natural Bond Orbital Analysis

We examined the frontier molecular orbitals (MOs) of **4**-**6** at the B3LYP/6-311++G(d,p) level of theory, inclusive of acetonitrile solvent (Figure 6). The nature of the HOMO and LUMO are relatively consistent for isomers of **4**, **5** and **6**. In **4** the HOMO has a π–type contribution from the central C=C double bond as well as delocalization into the π systems of both rings for both isomers. The LUMO is a π* symmetric orbital dominated by bonding contributions between the imidazole rings and the central C=C unit. In dicationic **5** the distribution of the HOMO and LUMO is similar to **4** for both isomers, except that the non-planar character of the rings reduces the contribution from the central C=C unit in the HOMO of **5**. For cationic **6** the HOMO for both isomers has π character, primarily on the neutral imidazole ring (with an asymmetric contribution from the central C=C bond that largely arises from C(2) pπ), while the LUMO is more evenly distributed over the two rings. NBOs at the same level of theory indicate a greater population of the C(1)-C(2) π orbital in **Z-6** (1.90 e) compared to **E-6** (1.81 e), consistent with an increased Wiberg bond index (WBI) of the C=C bond in **Z-6** (1.76 compared to 1.64 in **E-6**), and greater bond localization in **Z-6**. Occupation of C(2)-C(4) and C(3)-C(1) σ NBOs similarly reflects greater delocalization (and increased WBI) in **E-6**. WBIs and NBO occupations are provided in the Supporting Information.

In all three sets of compounds the HOMO-LUMO gap for the Z-isomer is larger than that for the E-isomer (see Figure 5 for plots of frontier MOs). The difference in HOMO-LUMO gaps between the Z and E isomers is 0.37 and 0.27 eV for **4** and **5**, respectively, but is significantly larger for **6** at 0.72 eV. The greater HOMO-LUMO gap difference between E and Z isomers of **6** arises from both an increased HOMO-LUMO gap in **Z-6** and reduced gap in **E-6** compared to **4** and **5**, which may in part be attributed to the asymmetry and electron density localization of **6** (and the respective contributions of the central C=C to the HOMO/LUMO). The observation of greater orbital localization in **6** is consistent with the results of varying the proportion of HF exchange in the density functional (see above), which indicated that charge transfer and electron localization effects were greatest in **6**.

One possible suggestion is that the stabilization of the **Z-6** isomer is due to an n → π* interaction between the imidazole nitrogen lone pair and the cationic imidazolium ring in **Z-6**. However, while the distance of the imidazole nitrogen to the ring atoms and the centroid is consistent with reported separations for such interactions,[30] NBO calculations indicate an absence of orbital interactions between the imidazole nitrogen lone pair and the overall imidazolium ring. Nevertheless, NBO analysis indicates a donor-acceptor stabilization of *ca*. 10 kJ/mol between the imidazole nitrogen lone pair (N1) and a p-character π∗ orbital on C(4).

	E-4	E-5	E-6
LUMO	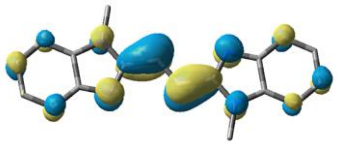	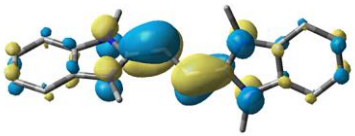	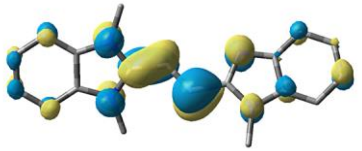
	E = -2.24 eV	E = -3.25 eV	E = -2.84 eV
HOMO	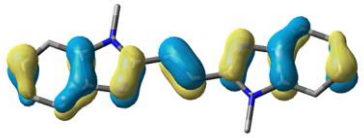	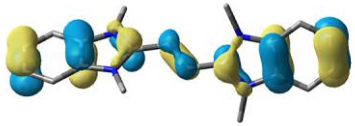	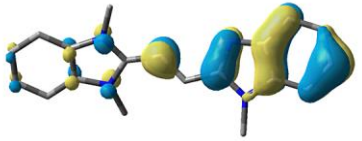
	E = -5.76 eV (H-L 3.52 eV)	E = -6.91 eV (H-L 3.66eV)	E = -6.19 eV (H-L 3.35 eV)
	Z-4	**Z-5**	**Z-6**
LUMO	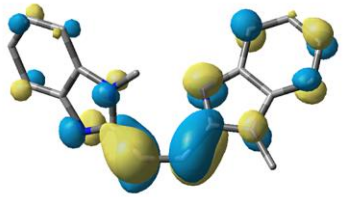	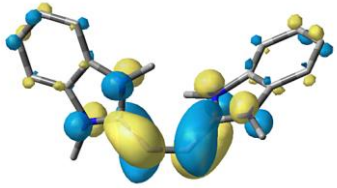	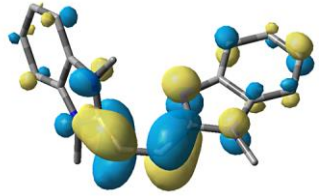
	E = -2.06 eV	E = -3.12 eV	E = -2.30 eV
HOMO	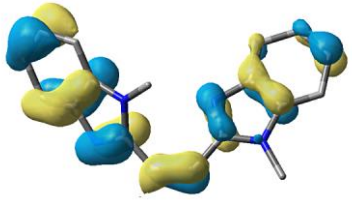	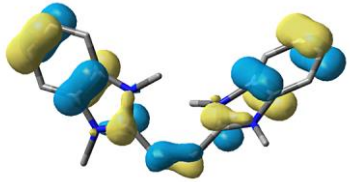	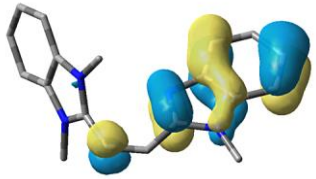
	E = -5.94 eV (H-L 3.89 eV)	E = -7.04 eV (H-L 3.93 eV)	E = -6.37 eV (H-L 4.07 eV)

Figure 5. Frontier molecular orbitals, orbital energies (eV) and HOMO-LUMO gaps (H-L, eV) of compounds **4-6**. B3LYP/6-311++G(d,p) results inclusive of acetonitrile solvent at B3LYP/6-311++G(d,p) gas phase geometries.

Electron density analysis

Analysis of the electron density with the QTAIM[31] approach indicates a non-covalent N(1)-C(4) interaction in **Z-6** (Figure 6), indicated by bond paths (lines) and bond critical points (BCP, red dots). Following the approach of Jenkins,[32] we have taken a physics-inspired approach to explore the presence of cis and trans effects in **4**-**6**. The cis effect is related to the tendency of electronic density to move away from the BCP towards the associated nuclear attractors, which may be quantified by the largest positive (λ_3) eigenvalue of the Hessian matrix of the electronic density (ρ) at the BCP. Jenkins noted that the physical origin of the cis effect is related to the central C=C bond path being more bent and having lower ellipticity in the cis isomer.[32]

For **4**-**6**, QTAIM analysis (Figure 6) indicates that the central C=C bond-path in the Z isomer is more highly curved (defined as the difference between the bond-path length and the internuclear separation). Bond-path curvature, favouring Z, is at a maximum for **6**. Analysis of λ_3^{cis} - λ_3^{trans} pairs (excluding the central C=C BCP) allows a bond-by-bond analysis of Z and E-stability contributions. Positive values indicate Z-stability while negative values indicate E-stability. Each of **4**-**6** exhibits both Z and E-stabilizing interactions. For **4**, there is an overall equal contribution of Z (0.148) and E (-0.148) stabilizing bond paths, while for **5** the E-stabilizing interactions (-0.126) are greater than the Z-stabilizing interactions (0.059). For **6** the Z-stabilizing interactions (0.246) are greater than those for E (-0.115). While the presence of both Z and E-effects in each isomer does not allow a definitive statement of the presence of a cis-effect in **6**, it may be concluded that there is a greater cis-effect in **6** compared to **4**-**5**.

Intramolecular symmetry-adapted perturbation theory (I-SAPT) analysis was employed to investigate intramolecular interactions between the benzimidazole rings in **4**-**6** (results provided in Supporting Information). In each case, the interacting fragments were defined as the benzimidazole rings, while the central C_2H_2 was the linking unit. The I-SAPT interaction energy may be partitioned into electrostatic,

exchange, induction and dispersion contributions. In the present work, the Z-E difference in interaction energy (and components) is the most relevant quantity. For **4** and **5**, the Z-E difference in overall I-SAPT energy is *ca*. +35 kJ/mol, whereas for **6** it is -0.3 kJ/mol. Interestingly, the dispersion contribution consistently favours the Z isomer of each of **4**-**6** by about 14 kJ/mol, while the exchange contribution favours the E isomer by 17.8 (**4**), 6.1 (**5**) and 14.5 kJ/mol (**6**). For **6** these two contributions largely cancel, which together with the relatively small induction effect, results in only a small difference in I-SAPT energies between **E-6** and **Z-6**. For **4**-**5** the E-Z difference in I-SAPT energies is dominated by electrostatics (32.6 compared to total difference of 35.7 kJ/mol for **4** and 46.3 compared to total difference of 35.3 kJ/mol for **5**), which serves to favour the E isomer. In **E-4** the electrostatic interaction is actually attractive (**Z-4** is repulsive), whereas in **5** the electrostatic repulsion is large, and greatest for the Z isomer.

The combination of QTAIM and I-SAPT analysis indicates that electrostatic interactions are the most significant factor behind the observed cis-effect in **6**.

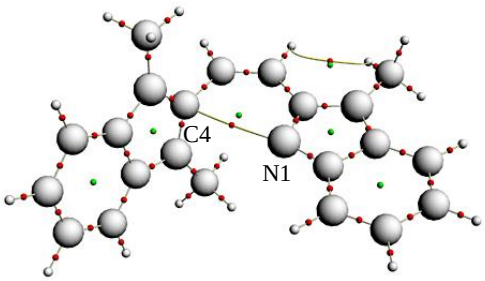

Figure 6. QTAIM illustration of non-covalent interactions in **Z-6**. Electron density from MP2/6-311G(d,p) calculation, inclusive of acetonitrile solvent.

Luminescence

The absorption and photoluminescence spectra obtained from pure samples of the **E-6** and **Z-6** isomers dissolved in acetonitrile (298 K) are shown in Figure 7. The absorption spectrum of the E-isomer is characterized by an intense band at 363 nm (ε = 50,802 M^{-1} cm^{-1}), whereas the Z-isomer has a less intense band at 329 nm (ε = 16,027 M^{-1} cm^{-1}). In both cases the peaks are assigned to $\pi \rightarrow \pi^*$ transitions and have a similar wavelength-dependence to the gas-phase PISA spectra presented in Figure 4. CAM-B3LYP/6-31+G(d) TD-DFT calculations (acetonitrile solvent) give absorbance maxima at 368 nm (**E-6**) and 308 nm (**Z-6**) for singlet excitations described as HOMO $\rightarrow$ LUMO transitions, in reasonable agreement with experiment. The trend is consistent with the hypsochromic shift of the absorption spectra for the two isomers.

Figure 7 also shows the fluorescence spectra obtained for pure samples of **E-6** and **Z-6** dissolved in acetonitrile following excitation at 350 nm. Irrespective of the starting isomer, the resulting fluorescence profiles were identical, with maxima at 487 nm. The apparent fluorescence quantum yields were found to be very similar for the two samples; 0.037±0.001 for **E-6** and 0.031±0.004 for **Z-6**.

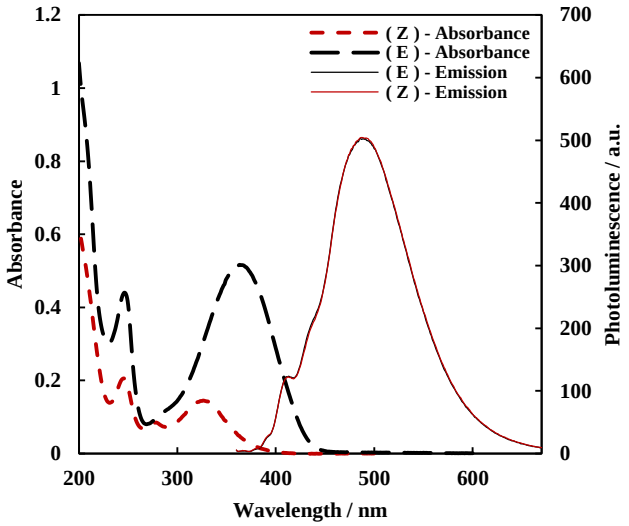

Figure 7. Photoluminescence (solid lines) and absorption (dashed lines) spectra of 10 μM solutions of **E-6** and **Z-6** in acetonitrile at 298 K. $\lambda_{excitation}$ = 350 nm).

These observations suggest the rapid establishment of a cis-dominated photostationary state, regardless of the starting condition, noting that the trans species is expected to be significantly less emissive due to the competing isomerization process. Further evidence for this is provided by the observation that, despite the difference in absorption profiles between the samples, **E-6** and **Z-6** solutions produce identical excitation spectra, with a λ_{max} of 349 nm. We speculate that an ultrafast rearrangement, proceeding via a twisted excited intermediate is responsible for the Z-E isomerization, as is well established for excited state isomerization of stilbene (Figure 8).[33]

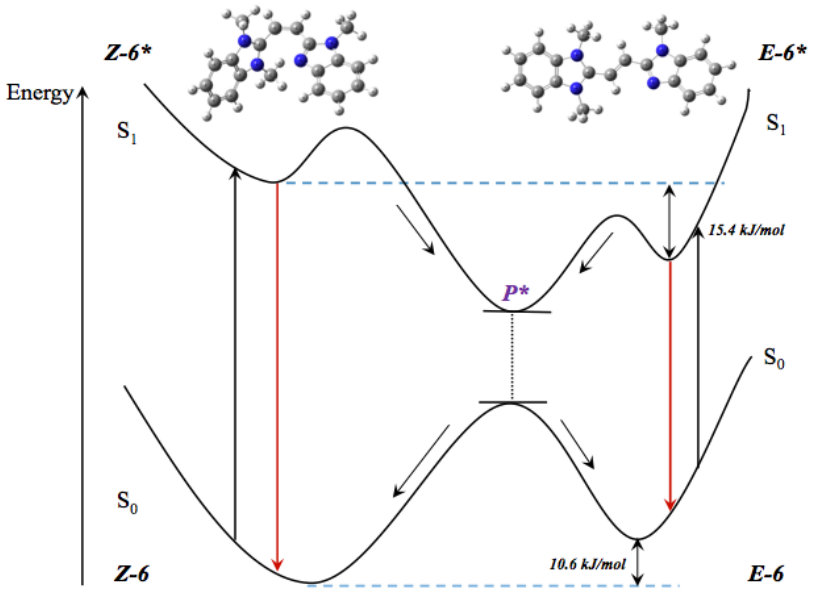

Figure 8. Schematic energy diagram for conversion between **E-6** and **Z-6** isomers, where *P** is a twisted excited intermediate with a perpendicular geometry. Energy difference between S_0 states of **Z-6** and **E-6** is 10.6 kJ/mol (DLPNO-CCSD(T)/cc-pVTZ including solvent). The S_1 state of **E-6** is lower than the S_1 state of **Z-6** by 15.4 kJ/mol from gas phase CASSCF(4,5)/cc-pVTZ calculations.

4. Conclusions

In summary, we have discovered the first alkene with two carbon bound substituents where the Z-isomer has a greater thermodynamic stability than the E-isomer. The effect persists in the gas-phase and in solution as characterised by gas phase ion mobility studies and observed in the bulk material. The underlying rationale for the preference for the Z-isomer in **6** arises from non-covalent (electrostatic) interactions between the N lone pair of the benzimidazole cation and the central C of the benzimidazolium, and an increased localization of the central C=C double bond in the Z-isomer for the cation. In dicationic **5** no lone pair is available, and in **4** the neutral imidazole ring likely has a lowered electrophilicity. Thus the presence of the heteroatoms is the key factor in making the Z-isomer more stable for **6**, in the lone pair bearing imidazole and cationic imidazolium ring allowed for by the nitrogen atoms that would not be found in a purely organic diaryl alkene.

Supporting Information. Experimental details. NMR and mass spectra. Cartesian coordinates of optimized geometries. CCDC 1511550 and 1511551 contain the supplementary crystallographic data for this paper. These data are provided free of charge by The Cambridge Crystallographic Data Centre.

Corresponding Authors

*j.dutton@latrobe.edu.au

*david.wilson@latrobe.edu.au

ACKNOWLEDGMENT

We thank the La Trobe Institute for Molecular Sciences, Melbourne University and the Australian Research Council (JLD, DE130100186, FT160100007; EJB DP150101427 and DP160100474) for their generous funding of this project. We acknowledge generous allocations of computing from La Trobe University, Intersect, and NCI.

TOC Synopsis and Figure

In this study we report on the first example of an acyclic diorganoalkene (i.e. a stilbene analogue) where the Z isomer is more stable than the E isomer. The root of the unusual stability of the Z isomer is traced to a non-covalent interaction between the neutral imidazole and the cationic imidazolium ring.

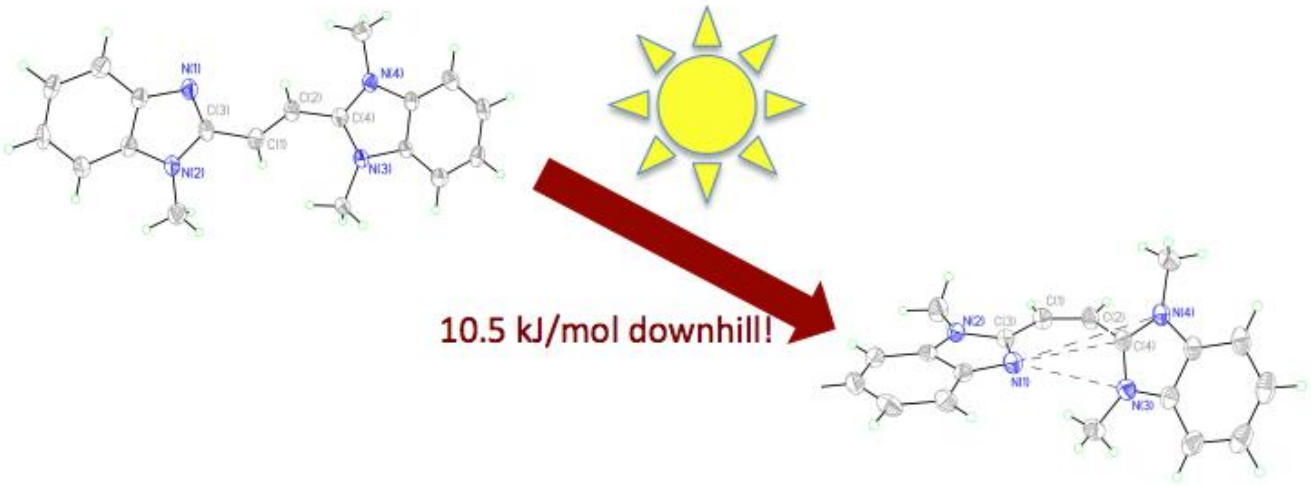

References

[1] (a) N. C. Craig, E. A. Entemann, *J. Am. Chem. Soc.* **1961**, *83*, 3047; (b) N. C. Craig, L. G. Piper, V. L. Wheeler, *J. Phys. Chem.* **1971**, *75*, 1453; (c) J. T. Waldron, W. H. Snyder, *J. Am. Chem. Soc.* **1973**, *95*, 5491; (d) R. C. Bingham, *J. Am. Chem. Soc.* **1976**, *98*, 535; (e) J. S. Binkley, J. A. Pople, *Chemical Physics Letters* **1977**, *45*, 197; (f) K. B. Wiberg, M. A. Murcko, K. E. Laidig, P. J. MacDougall, *J. Phys. Chem.* **1990**, *94*, 6956; (g) K. B. Wiberg, C. M. Hadad, C. M. Breneman, K. E. Laidig, M. A. Murcko, T. J. Lerpage, *Science* **1991**, *252*, 1266; (h) R. Kanakaraju, K. Senthilkumar, P. Kolandaivel, *J. Mol. Struct.(THEOCHEM)* **2002**, *589–590*, 95; (i) D. Feller, K. A. Peterson, D. A. Dixon, *J. Phys. Chem. A.* **2011**, *115*, 1440; (j) D. Banerjee, A. Ghosh, S. Chattopadhyay, P. Ghosh, R. K. Chaudhuri, *Molecular Physics* **2014**, *112*, 3206; (k) J. N. Butler, R. D. McAlpine, *Can. J. Chem.* **1963**, *41*, 2487; (l) K. E. Harwell, L. F. Hatch, *J. Am. Chem. Soc.* **1955**, *77*, 1682; (m) J. W. Crumb, *J. Org. Chem.* **1963**, *28*, 953; (n) D. Feller, N. C. Craig, P. Groner, D. C. McKean, *J. Phys. Chem. A.* **2011**, *115*, 94; (o) R. K. Chaudhuri, J. F. Hammond, K. F. Freed, S. Chattopadhyay, U. S. Mahapatra, *J. Chem. Phys.* **2008**, *129*, 064101.

[2] (a) R. B. Bates, W. A. Beavers, *J. Am. Chem. Soc.* **1974**, *96*, 5001; (b) P. v. R. Schleyer, J. Kaneti, Y. Wu, J. Chandrasekhar, *J. Organomet. Chem.* **1992**, *426*, 143.
[3] (a) A. D. Becke, *Phys. Rev. A* **1988**, *38*, 3098; (b) C. Lee, W. Yang, R. G. Parr, *Phys. Rev. B: Condens. Matter* **1988**, *37*, 785.
[4] K. Raghavachari, J. S. Binkley, R. Seeger, J. A. Pople, *J. Chem. Phys.* **1980**, *72*, 650.
[5] M. J. Frisch, G. W. Trucks, H. B. Schlegel, G. E. Scuseria, M. A. Robb, J. R. Cheeseman, G. Scalmani, V. Barone, B. Mennucci, G. A. Petersson, H. Nakatsuji, M. Caricato, X. Li, H. P. Hratchian, A. F. Izmaylov, J. Bloino, G. Zheng, J. L. Sonnenberg, M. Hada, M. Ehara, K. Toyota, R. Fukuda, J. Hasegawa, M. Ishida, T. Nakajima, Y. Honda, O. Kitao, H. Nakai, T. Vreven, J. J. A. Montgomery, J. E. Peralta, F. Ogliaro, M. Bearpark, J. J. Heyd, E. Brothers, K. N. Kudin, V. N. Staroverov, R. Kobayashi, J. Normand, K. Raghavachari, A. Rendell, J. C. Burant, S. S. Iyengar, J. Tomasi, M. Cossi, N. Rega, J. M. Millam, M. Klene, J. E. Knox, J. B. Cross, V. Bakken, C. Adamo, J. Jaramillo, R. Gomperts, R. E. Stratmann, O. Yazyev, A. J. Austin, R. Cammi, C. Pomelli, J. W. Ochterski, R. L. Martin, K. Morokuma, V. G. Zakrzewski, G. A. Voth, P. Salvador, J. J. Dannenberg, S. Dapprich, A. D. Daniels, Ö. Farkas, J. B. Foresman, J. V. Ortiz, J. Cioslowski, D. J. Fox, Gaussian 09, Revision E.01, Gaussian, Inc., Wallingford CT, **2013**.
[6] S. Grimme, S. Ehrlich, L. Goerigk, *J. Comp. Chem.* **2011**, *32*, 1456.
[7] E. D. Glendening, J. K. Badenhoop, A. E. Reed, J. E. Carpenter, J. A. Bohmann, C. M. Morales, F. Weinhold, NBO 5.9 (http://www.chem.wisc.edu/~nbo5), Theoretical Chemistry Institute, University of Wisconsin, Madison, WI, **2011**.
[8] (a) C. Pomelli, J. Tomasi, V. Barone, *Theor. Chim. Acta* **2001**, *105*, 446; (b) E. Cances, B. Mennucci, J. Tomasi, *J. Chem. Phys.* **1997**, *107*, 3032; (c) J. Tomasi, B. Mennucci, E. Cances, *J. Mol. Struct. (THEOCHEM)* **1999**, *464*, 211.
[9] A. V. Marenich, C. J. Cramer, D. G. Truhlar, *J. Phys. Chem. B* **2009**, 6378.
[10] C. Riplinger, F. Neese, *J. Chem. Phys.* **2013**, 034106.
[11] T. H. Dunning Jr., *J. Chem. Phys.* **1989**, *90*, 1007.
[12] F. Neese, *WIREs: Comput. Mol. Sci.* **2012**, *2*, 73.
[13] S. Sinnecker, A. Rajendran, A. Klamt, M. Diedenhofen, F. Neese, *J. Phys. Chem. A* **2006**, *110*, 2235.
[14] (a) H.-J. Werner, P. J. Knowles, G. Knizia, F. R. Manby, M. Schütz, P. Celani, W. Györffy, D. Kats, T. Korona, R. Lindh, A. Mitrushenkov, G. Rauhut, K. R. Shamasundar, T. B. Adler, R. D. Amos, A. Bernhardsson, A. Berning, D. L. Cooper, M. J. O. Deegan, A. J. Dobbyn, F. Eckert, E. Goll, C. Hampel, A. Hesselmann, G. Hetzer, T. Hrenar, G. Jansen, C. Köppl, Y. Liu, A. W. Lloyd, R. A. Mata, A. J. May, S. J. McNicholas, W. Meyer, M. E. Mura, A. Nicklaß, D. P. O'Neill, P. Palmieri, D. Peng, K. Pflüger, R. Pitzer, M. Reiher, T. Shiozaki, H. Stoll, A. J. Stone, R. Tarroni, T. Thorsteinsson, M. Wang., Molpro 2015.1 (www.molpro.net), Cardiff, UK; (b) H.-J. Werner, P. J. Knowles, G. Knizia, F. R. Manby, M. Schütz, *WIREs Comput. Mol. Sci.* **2012**, *2*, 242.
[15] R. Bader, *Atoms in Molecules: A Quantum Theory*, Oxford University Press, USA, **1994**.
[16] T. A. Keith, AIMALL, 17.01.25 (aim.tkgristmill.com), TK Gristmill Software, Overland Park KS, USA, **2017**.
[17] (a) E. J. Baerends, T. Ziegler, A. J. Atkins, J. Autschbach, D. Bashford, A. Bérces, F. M. Bickelhaupt, C. Bo, P. M. Boerrigter, L. Cavallo, D. P. Chong, D. V. Chulhai, L. Deng, R. M. Dickson, J. M. Dieterich, D. E. Ellis, M. van Faassen, L. Fan, T. H. Fischer, C. Fonseca Guerra, M. Franchini, A. Ghysels, A. Giammona, S. J. A. van Gisbergen, A. W. Götz, J. A. Groeneveld, O. V. Gritsenko, M. Grüning, S. Gusarov, F. E. Harris, P. van den Hoek, C. R. Jacob, H. Jacobsen, L. Jensen, J. W. Kaminski, G. van Kessel, F. Kootstra, A. Kovalenko, M. V.

Krykunov, E. van Lenthe, D. A. McCormack, A. Michalak, M. Mitoraj, S. M. Morton, J. Neugebauer, V. P. Nicu, L. Noodleman, V. P. Osinga, S. Patchkovskii, M. Pavanello, C. A. Peeples, P. H. T. Philipsen, D. Post, C. C. Pye, W. Ravenek, J. I. Rodríguez, P. Ros, R. Rüger, P. R. T. Schipper, H. van Schoot, G. Schreckenbach, J. S. Seldenthuis, M. Seth, J. G. Snijders, M. Solà, M. Swart, D. Swerhone, G. te Velde, P. Vernooijs, L. Versluis, L. Visscher, O. Visser, F. Wang, T. A. Wesolowski, E. M. van Wezenbeek, G. Wiesenekker, S. K. Wolff, T. K. Woo, A. L. Yakovlev, ADF2016, (http://www.scm.com/), Theoretical Chemistry, Vrije Universiteit, Amsterdam, The Netherlands, **2016**; (b) G. te Velde, F. M. Bickelhaupt, E. J. Baerends, C. F. Guerra, S. J. A. v. Gisbergen, J. G. Snijders, T. Ziegler, *J. Comp. Chem.* **2001**, *22*, 931.

[18] J. G. Snijders, P. Vernooijs, E. J. Baerends, *Atomic Data and Nuclear Data Tables* **1981**, *26*, 483.

[19] J. Krijn, E. J. Baerends, in *Fit Functions in the HFS-Method: Internal Report (in Dutch)*, Vrije Universiteit Amsterdam, The Netherlands, **1984**.

[20] E. Van Lenthe, E. J. Baerends, J. G. Snijders, *J. Chem. Phys.* **1993**, *99*, 4597.

[21] J. M. Turney, A. C. Simmonett, R. M. Parrish, E. G. Hohenstein, F. Evangelista, J. T. Fermann, B. J. Mintz, L. A. Burns, J. J. Wilke, M. L. Abrams, N. J. Russ, M. L. Leininger, C. L. Janssen, E. T. Seidl, W. D. Allen, H. F. Schaefer III, R. A. King, E. F. Valeev, C. D. Sherrill, T. D. Crawford, *WIREs Comput. Mol. Sci.* **2012**, *2*, 556.

[22] E. Papajak, D. G. Truhlar, *J. Chem. Theory Comput.* **2011**, *7*, 10.

[23] (a) J. L. Dutton, D. J. D. Wilson, *Angew. Chem. Int. Ed.* **2012**, *51*, 1477; (b) D. C. Georgiou, B. D. Stringer, N. Holzmann, C. F. Hogan, P. J. Barnard, D. J. D. Wilson, G. Frenking, J. L. Dutton, *Chem. Eur. J.* **2015**, *21*, 3377.

[24] (a) D. D. Dalgatov, A. M. Simonov, *Zh. Obsch. Khim. (English translation)* **1963**, *33*, 996; (b) F. A. Binningen, A. Siegrist, *Vol. 2,808,407* (Ed.: U. P. Office), United States of America, **1957**.

[25] B. D. Adamson, N. J. A. Coughlan, P. B. Markworth, R. E. Continetti, E. J. Bieske, *Rev. Sci. Instrum.* **2014**, *85*, 123109.

[26] F. Lanucara, S. W. Holman, C. J. Gray, C. E. Eyers, *Nat. Chem.* **2014**, *6*, 281.

[27] N. J. A. Coughlan, M. S. Scholz, C. S. Hansen, A. J. Trevitt, B. D. Adamson, E. J. Bieske, *J. Am. Soc. Mass Spectrom.* **2016**, *27*, 1483.

[28] (a) N. A. Pierson, S. J. Valentine, D. E. Clemmer, *J. Phys. Chem. B* **2010**, *114*, 7777; (b) N. A. Pierson, D. E. Clemmer, *Int. J. Mass Spectrom.* **2015**, *377*, 646.

[29] T. A. Baker, M. Head-Gordon, *J. Phys. Chem. A* **2010**, *114*, 10326.

[30] T. J. Mooibroek, P. Gamez, J. Reedijk, *CrystEngComm* **2008**, *10*, 1501.

[31] R. F. Bader, *Atoms in Molecules: A Quantum Theory; Oxford University Press* **1994**.

[32] S. Jenkins, S. R. Kirk, C. Rong, D. Yin, *Mol. Physics* **2013**, *111*, 793.

[33] (a) P. de Mayo, *Vol. 3*, Academic Press, New York, **1980**; (b) J. S. Baskin, L. Banares, S. Pedersen, A. H. Zewail, *J. Phys. Chem.* **1996**, *100*, 11920.